12

Optimal Design of an Hybrid Wind-Diesel System with Compressed Air Energy Storage for Canadian Remote Areas

Younes Rafic[1], Basbous Tammam[2] and Ilinca Adrian[3]
[1]*Lebanese University, Faculty of Engineering, Beirut,*
[2]*LREE, University of Quebec in Chicoutimi, Chicoutimi,*
[3]*LREE, Quebec University in Rimouski, Rimouski,*
[1]*Lebanon*
[2,3]*Canada*

1. Introduction

1.1 Context

Most of the remote and isolated communities or technical installations (communication relays, meteorological systems, tourist facilities, farms, etc.) which are not connected to national electric distribution grids rely on Diesel engines to generate electricity [1]. Diesel-generated electricity is more expensive in itself than large electric production plants (gas, hydro, nuclear, wind) and, on top of that, should be added the transport and environmental cost associated with this type of energy.

In Canada, approximately 200,000 people live in more than 300 remote communities (Yukon, TNO, Nunavut, islands) and are using Diesel-generated electricity, responsible for the emission of 1.2 million tons of greenhouse gases (GHG) annually [2]. In Quebec province, there are over 14,000 subscribers distributed in about forty communities not connected to the main grid. Each community constitutes an autonomous network that uses Diesel generators.

In Quebec, the total production of Diesel power generating units is approximately 300 GWh per year. In the mean time, the exploitation of the Diesel generators is extremely expensive due to the oil price increase and transportation costs. Indeed, as the fuel should be delivered to remote locations, some of them reachable only during summer periods by barge, the cost of electricity produced by Diesel generators reached in 2007 more than 50 cent/kWh in some communities, while the price for selling the electricity is established, as in the rest of Quebec, at approximately 6 cent/kWh [3].

The deficit is spread among all Quebec population as the total consumption of the autonomous grids is far from being negligible. In 2004, the autonomous networks represented 144 MW of installed power, and the consumption was established at 300 GWh. Hydro-Quebec, the provincial utility, estimated at approximately 133 millions CAD$ the annual loss, resulting from the difference between the Diesel electricity production cost and the uniform selling price of electricity [3].

Moreover, the electricity production by the Diesel is ineffective, presents significant environmental risks (spilling), contaminates the local air and largely contributes to GHG emission. In all, we estimate at 140,000 tons annual GHG emission resulting from the use of Diesel generators for the subscribers of the autonomous networks in Quebec. This is equivalent to GHG emitted by 35,000 cars during one year.

The Diesel power generating units, while requiring relatively little investment, are generally expensive to exploit and maintain, particularly when are functioning regularly at partial load [4]. The use of Diesel power generators under weak operating factors accelerates wear increases fuel consumption [5]. Therefore, the use of hybrid systems, which combine renewable sources and Diesel generators, allows reducing the total Diesel consumption, improving the operation cost and environmental benefits.

1.2 Wind-Diesel systems

Among all renewable energies, the wind energy experiences the fastest growing rate, at more than 30% annually for the last 5 years [7,8]. Presently, wind energy offers cost effective solutions for isolated grids when coupled with Diesel generators. The "Wind-Diesel hybrid system" (WDS) represent a technique of generation of electrical energy by using in parallel one or several wind turbines with one or several Diesel groups. This approach is at present used in Nordic communities in Yukon [9], Nunavut [10] and in Alaska [11].

The "penetration rate" is used in reference to the rated capacity of the installed wind turbines compared to the maximum and minimum loads. A strict definition of a "low-penetration" system is one when the maximum rated capacity of the wind component of the system does not exceed the minimum load of the community. In practical terms however, a low-penetration system is one where the wind turbines are sized so as not to interfere with the Diesel generators' ability to set the voltage and frequency on the grid. In effect, the wind-generated electricity is "seen" by the Diesel plant as a negative load to the overall system. It is important to note however that because such a system needs to be designed for the peak capacity of the wind generator it will typically operate with an average annual output of 20-35% of its rated power, such that while low-penetration systems will have noticeable fuel and emissions savings they will be fairly minor [12,2]. In many cases it is likely that similar savings could be achieved through energy efficiency upgrades for similar capital costs.

A "high-penetration" system without storage [13], as illustrated in Figure 1, is one where the output from the wind generators frequently exceeds the maximum load for extended periods of time (10 min to several hours), such that the Diesel generators can be shut off completely when there is significant wind. The variation of wind and Diesel-generated power according to the wind speed and considering a constant load is illustrated at Figure 2. The Diesel generators therefore are required only during periods of low winds and/or to meet peak demands. The advantage of such systems are that very significant fuel savings can be achieved reducing import and storage costs, but also will extend the life and servicing frequency of the Diesel generators as they will log less hours. Such systems can also benefit from economies of scale for construction and maintenance, but require much more significant and expensive control systems [14,15] to regulate the grid frequency and voltage while the Diesel generators are turned off. A dump load is required during periods when the power from the wind turbines exceeds the demand in order to maintain system frequency and voltage [11].

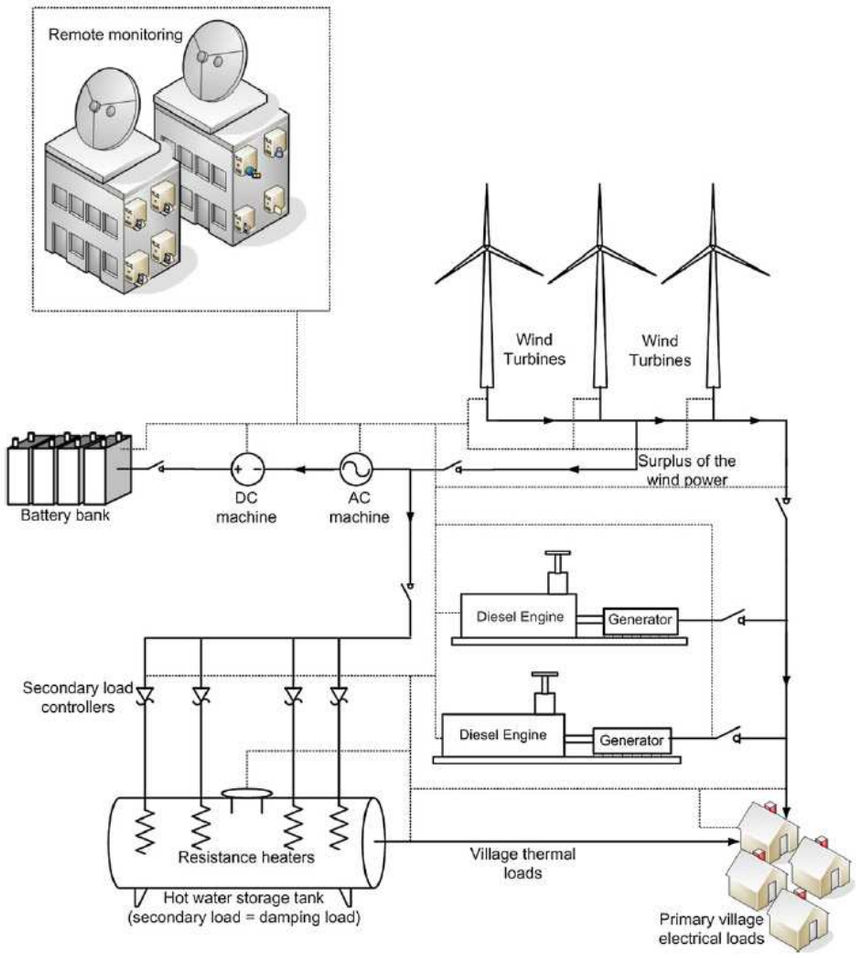

Fig. 1. Wind -Diesel system with dump load.

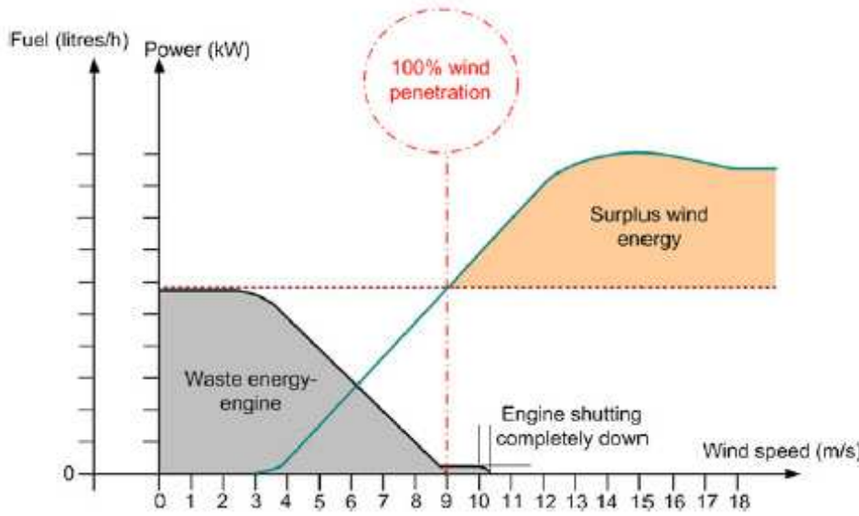

Fig. 2. Variation of wind and diesel power with wind speed for a high-penetration WDS [16].

A medium-penetration system refers to a system in between the low- and high-penetration configurations. A medium-penetration system will have periods of time when the wind-generated electricity dominates the Diesel-generated electricity and may also be able to meet the system load for brief periods of time (30 s - 5 min). When wind speeds are high and/or the community demand is very low, the Diesel generators may not be required at all, but are not shut off, rather they are left to idle to be able to respond quickly to load demands. A medium-penetration system is potentially subjected to both the benefits and the drawbacks of low- and high penetration configurations. Beyond a certain penetration, the obligation to maintain idle the Diesel at any time, generally around 25-30% of its nominal output power, forces the system to function at a very inefficient regime. Indeed, for low- and medium-penetration systems, the Diesel consumes, even without load, approximately 50% of the fuel at nominal power output. These systems are easier to implant but their economic and environmental benefits are marginal [12]. The use of high-penetration systems allows the stop of the thermal groups, ideally as soon as the wind power equals the instantaneous charge, to maximize the fuel savings. However, considering the Diesel starting time as well as the instantaneous charge and wind speed fluctuations, the thermal production must be available (Diesel group to minimal regime) from the moment when the over-production passes under a threshold, named power reserve, considered as security to answer to the instantaneous requested power. The value of this reserve should be chosen so that it insures the reliability of the system and has a direct effect on the fuel consumption and the exploitation and maintenance costs of the Diesel generators. In other words, the Diesels must still idle to compensate for a sudden wind power decrease under the level of the charge and a greater the value of the power reserve leads to longer periods of time during which the Diesels are functioning at inefficient regimes.

During time intervals when the excess of wind energy over the charge is considerable the Diesel engine must still be maintained on standby so that it can quickly respond to a wind speed reduction (reduce the time of starting up and consequent heating of the engine). This is an important source of over consumption because the engine could turn during hours without supplying any useful energy. Assuming optimum exploitation conditions [17,2] the use of energy storage with wind-Diesel systems can lead to better economic and environmental results, allows reduction of the overall cost of energy supply and increase the wind energy penetration rate (i.e., the proportion of wind energy as the total energy consumption on an annual basis) [2].

Presently, the excess wind energy is stored either as thermal potential (hot water), an inefficient way to store electricity as it cannot be transformed back in electricity when needed or in batteries which are expensive, difficult to recycle, a source of pollution (lead-acid) and limited in power and lifecycle. The fuel cells propose a viable alternative but due to their technical complexity, their prohibitive price and their weak efficiency, their appreciation in the market is still in an early phase. The required storage system should be easily adaptable to the hybrid system, available in real time and offer smooth power fluctuations. For this reason we examine the use of compressed air energy storage (CAES) with the wind-Diesel hybrid system (WDCAS), illustrated in Figure 3. The energy storage in the form of compressed air (CAES) is adaptable for the two sources of electricity production (wind energy and Diesel). Moreover, the CAES is an interesting solution to the

problem of strong stochastic fluctuations of the wind power because it offers a high efficiency conversion (60-70% for a complete charge-discharge cycle), uses conventional materials which are easy to recycle and is able to make an almost unlimited number of cycles [18,19].The compressed air energy storage can more specifically, be used to overcharge the Diesel engines and ensure maximum efficiency over all functioning regimes. In this paper we analyze the technical and economical performances of a Diesel engine overcharged with compressed produced from wind energy surpluses. However, the advantage of a hybrid system compared to a wind alone system, depends on many fundamental factors: the form and the type of the load, the regime and speed of the wind, the cost and the availability of energy, the relative cost of the wind machine, the storage system and other efficiency determining factors [20]. The capital cost of the wind turbine and the CAES system is considerably damped by the reduction of the operating costs of Diesel generators [21,22].

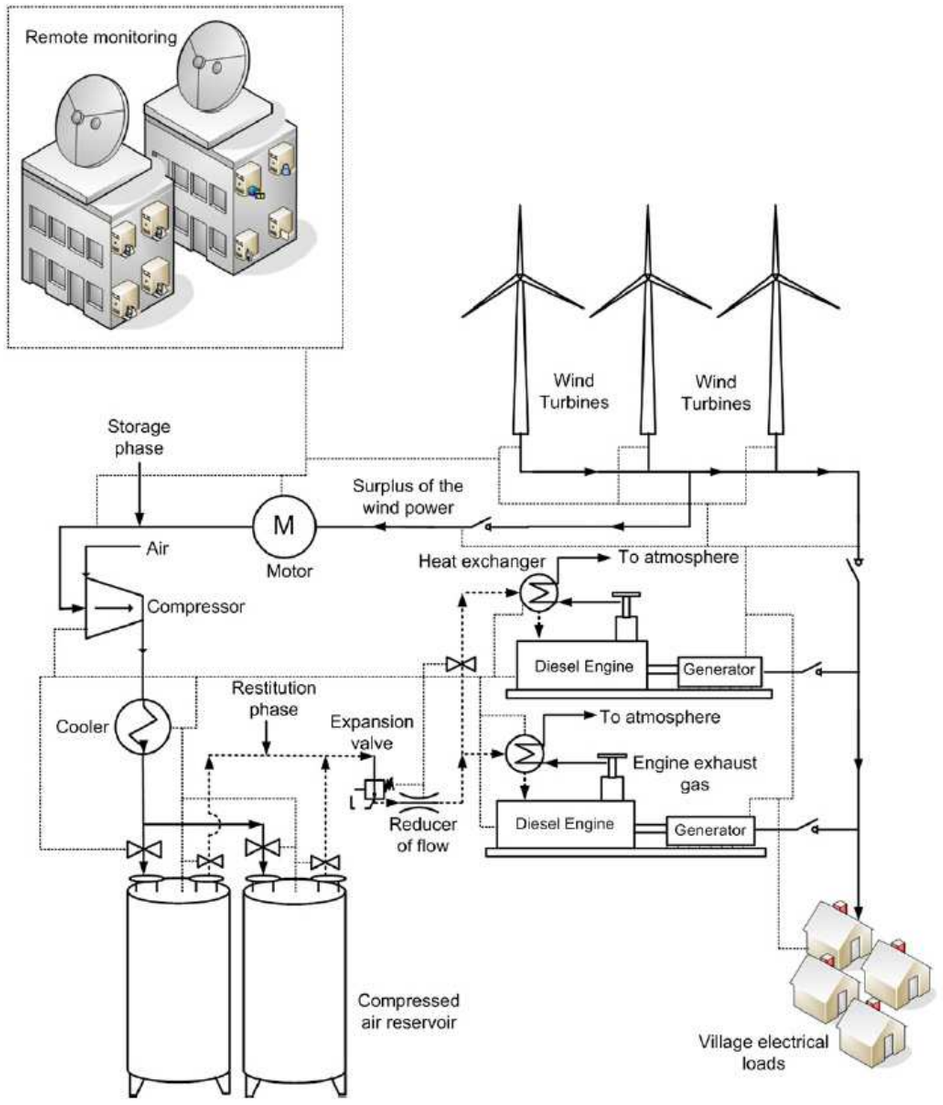

Fig. 3. Wind-Diesel system with compressed air energy storage

2. Suggested concept

2.1 Wind Diesel system with compressed air storage (WDCAS)

The proposed system, (WDCAS) combined with the Diesel engine supercharge, will increase of the rate of penetration of the wind energy (RPWE). The supercharging is a process which consists of a preliminary compression with an objective to raise the intake air density of engines to increase their specific power (power by swept volume) [23,24]. During periods of strong wind, the surplus of the wind power (when wind power penetration rate defined as quotient between the wind-generated power and the charge is greater than 1 e WPPR>1) is used to compress the air via a compressor and store it. The compressed air then serves to turbo-charge the Diesel engine with a dual advantage of increasing its power and decreasing the fuel consumption. The Diesel generator works during the periods of low wind velocity, when the wind power is not sufficient for the load.

The WDCAS has a very important commercial potential for remote areas as it is based on the use of Diesel generators already in place. It is conceived like the adaptation of the existing engines at the level of the intake system, the addition of a wind power station and an air compression and storage system. The lack of information on the economics, as well as on performances and reliability data of such systems is currently the main barrier to the acceptance of wind energy deployment in the remote areas. This project intends to answer some of these interrogations. Using information available [4,6,25], and performance analysis [23,26], we estimate that on a site with appreciable wind potential, the return on investment (ROI) for such installation is between 2 and 5 years, subject to the costs of fuel transport. For sites accessible only by helicopters the ROI can be less than a year [17]. This analysis does not take into account the raising prices of fuel, nor GHG credit which only tend to reduce the ROI [27].

2.2 Possible techniques for making advantage of CAES to increase Diesel engine efficiency

Among different techniques investigated, two of them were selected for being compatible with a simple adjustment of existing Diesel Power system without heavy investments:

Technique 1: admission of the compressed air at the compressor inlet

The indicated efficiency of a Diesel engine follows a quadratic variation function of Air-to-Fuel ratio, as shown in Figure 4. The idea is therefore to use the CAES to increase the pressure at the intake of the compressor, as shown in Figure 5, mainly at high loads, when there is a lack of air. This would increase the air flow admitted by the engine and increase therefore the Air-to-Fuel ratio to bring it artificially to its optimal value witch is around 53.

Technique 2: admission of the compressed air at the engine inlet

The idea is to remove the turbocharger and connect directly the CAES to the inlet of the engine, as shown in Figure 6. The benefit would be increasing the scavenging work to make it contributing to the provided power, in addition to the ability to increase the Air-to-Fuel ratio as in the previous technique.

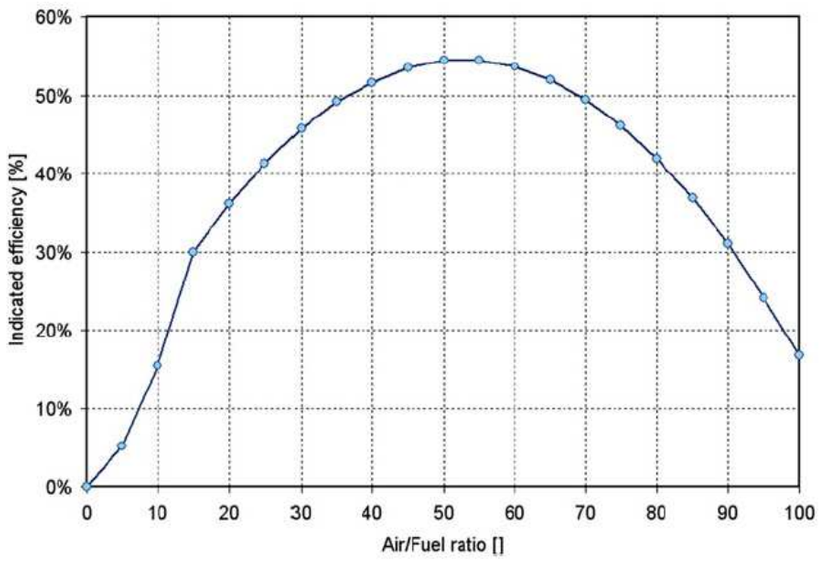

Fig. 4. Variation of indicated efficiency with the air/fuel ratio [39]

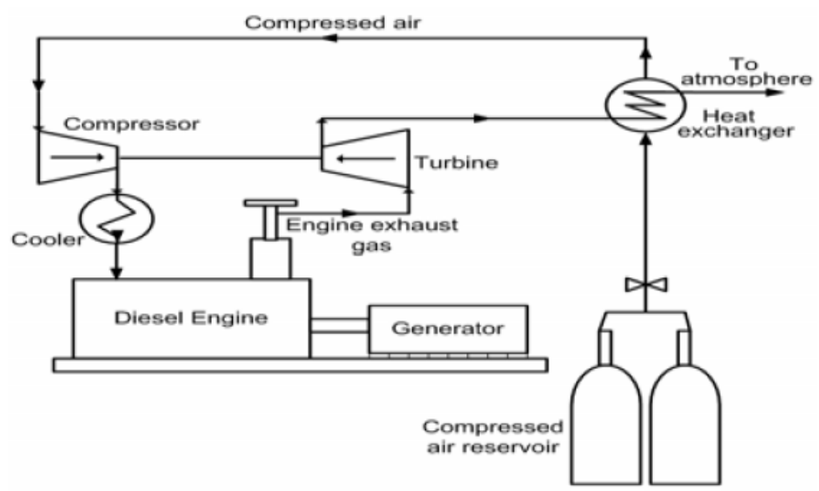

Fig. 5. Admission of CAES at the compressor intake.

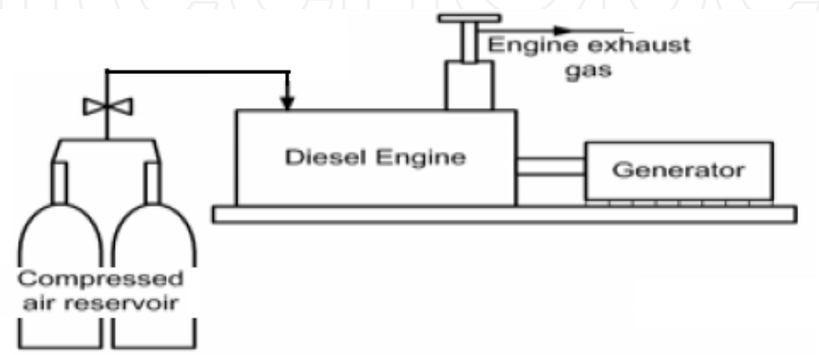

Fig. 6. Admission of CAES at the engine intake

3. Fuel economy evaluation by numerical analysis

3.1 Mathematical modeling

Technique 1

State variable	Can be expressed as a function of	Type	Reference
p_1	(p_0, Q_{comp})	Thermodynamic equation	
T_1	(p_o, T_o, p_1)	Thermodynamic equation	[37]
p_2	$(Q_{comp}, p_1, T_1, N_{comp})$	Thermodynamic equation	[37]
T_2	$(Q_{comp}, p_1, T_1, N_{comp})$	Thermodynamic equation	[37]
p_3	(Q_{comp}, p_2)	Thermodynamic equation	[37]
T_3	(Q_{comp}, p_2, T_2)	Empirical model	[37]
Q_{comp}	(p_2, p_3, N_{comp})	Cartography	[30]
η_{comp}	(p_2, p_3, N_{comp})	Cartography	[30]
P_{comp}	$(Q_{comp}, p_2, T_2, p_3, \eta_{comp})$	Thermodynamic equation	[30]
Q_{int}	(p_3, T_3, η_{vol})	Thermodynamic equation	[37]
η_{vol}	N_{eng}	Empirical model	[37, 39]
T_4	$(T_3, Q_{\text{int}}, Q_{fuel})$	Empirical model	[37]
P_{out}	$(Q_{fuel}, \eta_{ind}, P_{fric})$	Thermodynamic equation	[37]
P_{fric}	N_{eng}	Empirical model	[45]
η_{ind}	$(Q_{\text{int}}, Q_{fuel})$	Empirical model	[37, 39,40]
Q_{exh}	$(Q_{\text{int}}, Q_{fuel})$	Thermodynamic equation	[37]
Q_{turb}	(p_4, p_5, N_{turb})	Cartography	[30]
η_{turb}	(p_4, p_5, N_{turb})	Cartography	[30]
P_{turb}	$(Q_{turb}, p_4, T_4, p_5, \eta_{turb})$	Thermodynamic equation	[30]

The numerical resolution of the problem consists in finding the roots of the state variables which ensures the equilibrium of the system.

For an operation without CAES

The unknown variables are $\left(Q_{\text{int}}, Q_{fuel}, N_{comp}, p_3, p_4\right)$ and the equilibrium equations are the following:

- balance equation of the crankshaft:

The power supplied by the engine must be equal to the resistant power:

$$P_{out} = P_{load}$$

- balance equation of the turbocharger torque

The torque supplied by the turbine must be equal to the necessary torque to drive the compressor:

$$P_{comp} = P_{turb}$$

- balance equation of the turbocharger speed

The speed of the turbine and the compressor are equal:

$$N_{comp} = N_{turb}$$

- intake aire continuity

$$Q_{comp} = Q_{\text{int}}$$

- exhaust air continuity

$$Q_{turb} = Q_{exh}$$

For an operation with CAES

The unknown variables are $\left(Q_{\text{int}}, Q_{fuel}, N_{comp}, p_0, p_3, p_4\right)$ and the equilibrium equations are the same as previous five equations in addition to the sixth following equation:

- Optimal Air-to-Fuel ratio

$$\frac{Q_{\text{int}}}{Q_{fuel}} = 53$$

Technique 2

Main equations are issued from the mass and heat conservation as well as the ideal gas assumptions [6, 13]. The application of the first law or thermodynamics and the perfect gas law to the control volume results in the differential equation 1 [13] that drives all the thermodynamic transformations.

$$d\left(m \cdot u\right) = -P \cdot dV + dq_{\text{walls}} + dq_{\text{comb}} + h_T \cdot dm_{\text{int}} + h_{ech} \cdot dm_{\text{exh}} + h_{\text{fuel}} \cdot dm_{\text{fuel}} \quad (1)$$

State variable	Can be expressed as a function of	Type	Reference
u	(T, x_i)	Thermodynamic tables	[54]
h	(T, x_i)	Thermodynamic tables	[54]
V	θ	Kinematic equation	[56,57]
dq_{walls}	$(T_{gas}, T_{walls}, N_{eng})$	Empirical model	[55]
dq_{comb}	$(\theta, \theta_0, \theta_{delay})$	Empirical model	[56,57]
θ_{delay}	$(T_{gas}, P_{gas}, N_{eng})$	Chemical model	[56,57]
dm	$(P_{in}, P_{out}, T_{in}, A)$	Thermodynamic model	[56,57]

3.2 Results and analysis

Technique 1

We suppose in this numerical application that the used engine possesses a capacity of 5 l and turns at a regime of 1500 rotations per minute. Thus, the results obtained by the optimization are presented in Figures. 9-11. In conventional operation, the ratio air/fuel decreases with the load to reach in full load at the neighborhood of the stoichiometry as shown in Figure 9. For any requested torque lower than 120 Nm, we obtain an Air-to-Fuel ratio higher than 53, which means that there is no provision of the use of compressed air. Once the torque exceeds 120 N m, the turbocharger cannot ensure the quantity of necessary air to have an optimal air/fuel ratio. The engine then works in the zone of interest of operation with compressed air. Figure 10 shows the necessary inlet pressure of the compressor to operate the engine at its maximum efficiency thanks to the compressed air. Indeed, in the absence of CAES, the inlet pressure of the compressor is constant and equal to 1 bar, which is shown by the red curve ("Without Compressed Air"). The CAES allows feeding of the compressor at a chosen pressure to achieve the exact necessary air flow for maximum performance (efficiency). In our case, this pressure varies between 1 bar at very low regimes and 2.6 bars at full load. An adapted strategy for checking the valve relaxation of compressed air would achieve that balance. Finally, Figure 11 shows the reduction in fuel consumption which is brought about by the compressed air. This reduction in fuel consumption grows with the load to peak to 50% fuel saving at 800 Nm

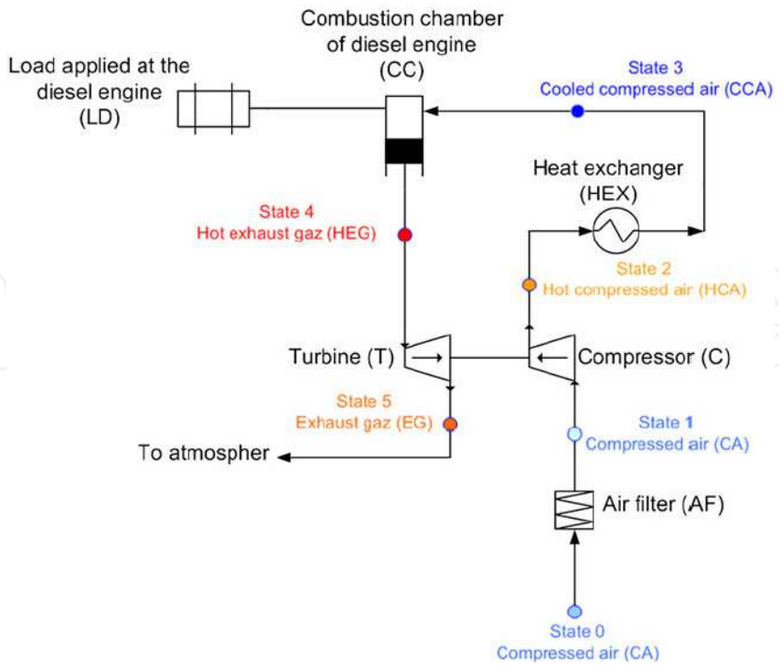

Fig. 7. Schema of Diesel engine main components

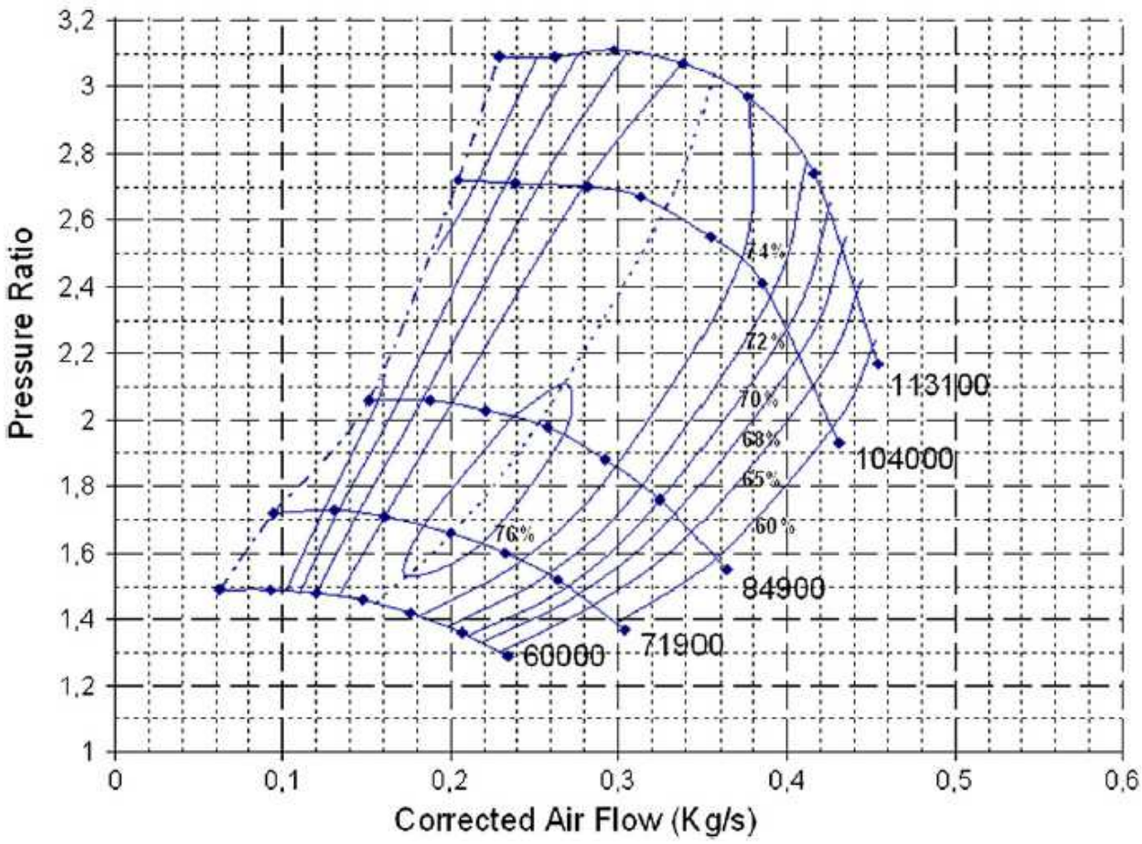

Fig. 8. Variation Characteristic curves of the compressor given by the manufacturer [30].

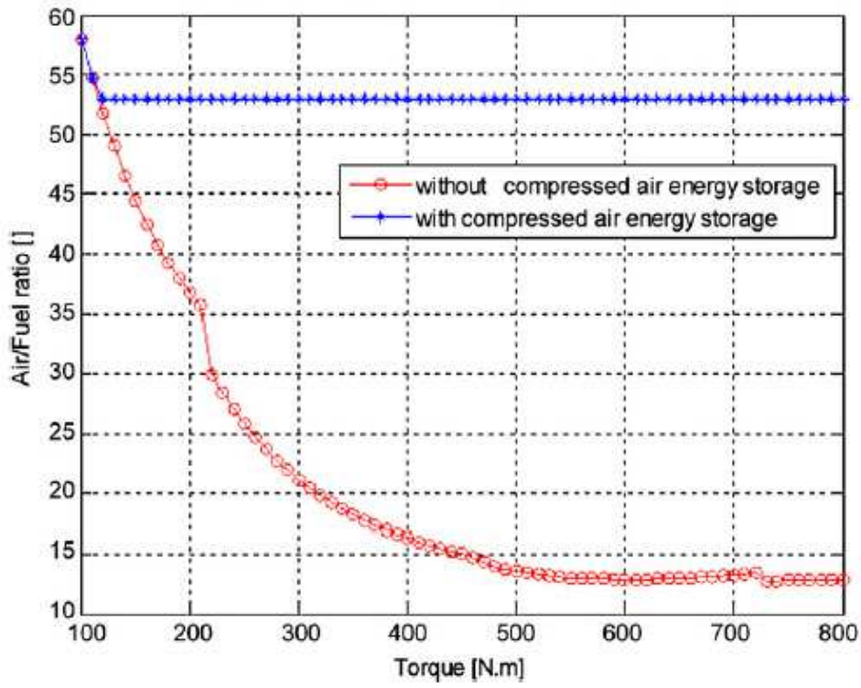

Fig. 9. Comparison of the (air/fuel) ratio.

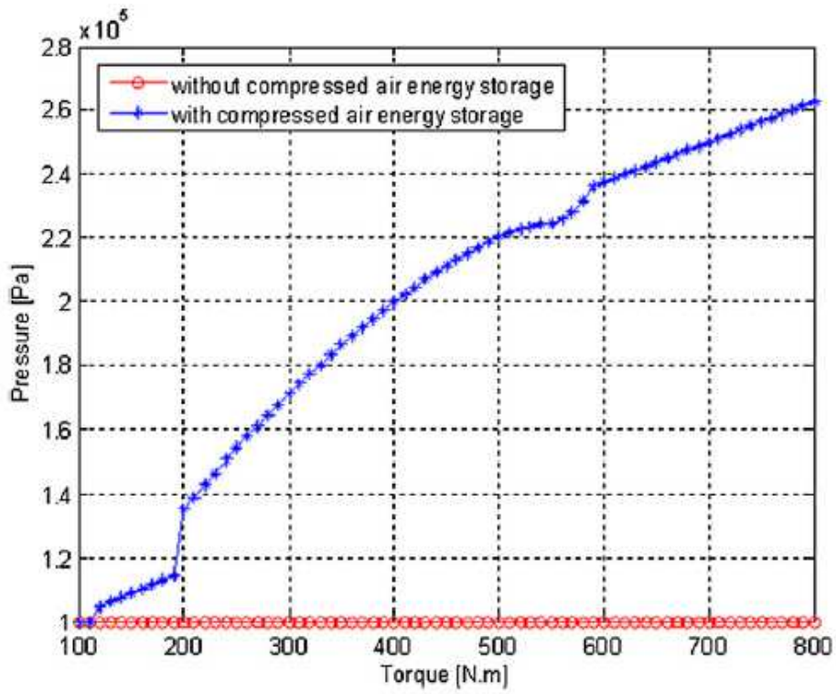

Fig. 10. Comparison of the pressure at compressor inlet..

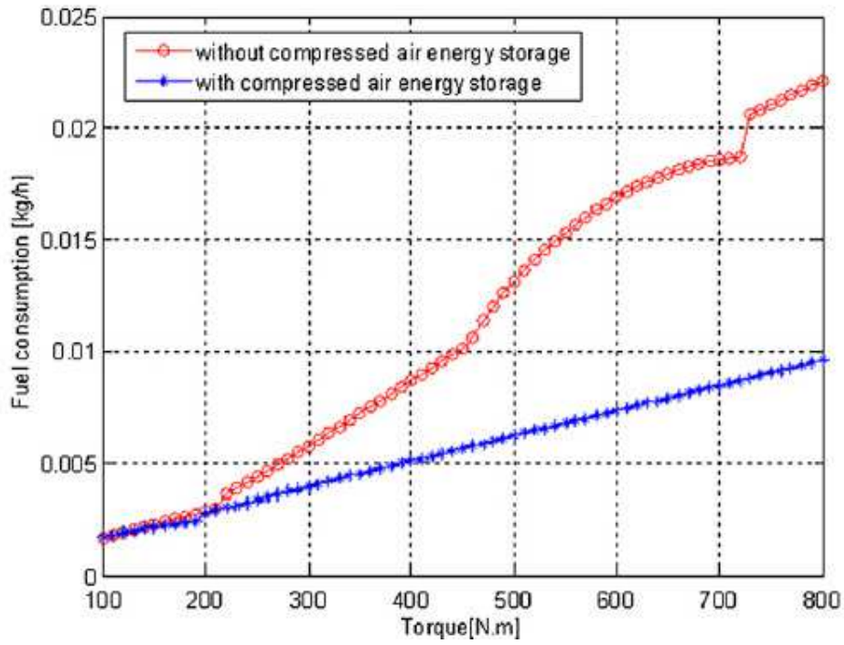

Fig. 11. Comparison of the fuel consumption.

Technique 2

In our study, we have chosen to focus on three operating modes to study the impact of injection advance:

- Turbocharged mode with compressed air cooling;
- CAES charged mode with an intake temperature of 25°C;
- CAES charged mode with an intake temperature of -50°C.

For the CAES charged mode temperatures, we know that a temperature drop will inevitably occur when expanding the CAES from storage pressure to intake pressure. However, it is possible to heat the intake air before admitting it using engine's cooling system or exhaust temperature recovery. We have chosen not to work below intake temperature of -50°C because it is the range of minimum external temperature that can be met in northern areas. Below this temperature, we need to investigate if the Diesel engine remains operational which exceeds the purpose of this study. These operating modes are not the only ones to be studied, but they were chosen to increase our understanding of the Diesel engine behavior regarding intake and exhaust conditions.

Detailed parametric study at BMEP = 10 bars

In order to understand its behavior, we will provide a complete analysis of the variation of the thermodynamic cycle and its efficiency, depending on the control parameters (intake pressure, intake temperature, exhaust pressure and injection advance) for a fixed load corresponding to a BMEP of 10 bars. Figure 13 illustrates the effect of intake pressure and exhaust pressure on specific fuel consumption of the engine at a BMEP of 10 bars for a fixed intake temperature of 298K and a fixed injection advance of 6 degrees. As we can observe, increasing intake pressure and reducing exhaust pressure highly reduces fuel consumption.

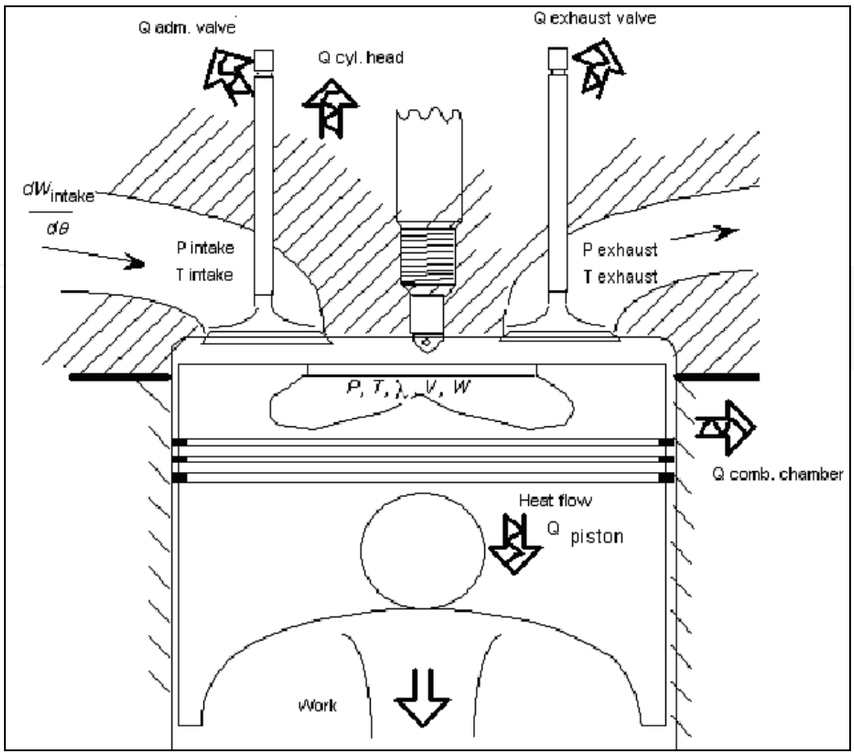

Fig. 12. Direct injection Diesel engine simplified thermodynamic model.

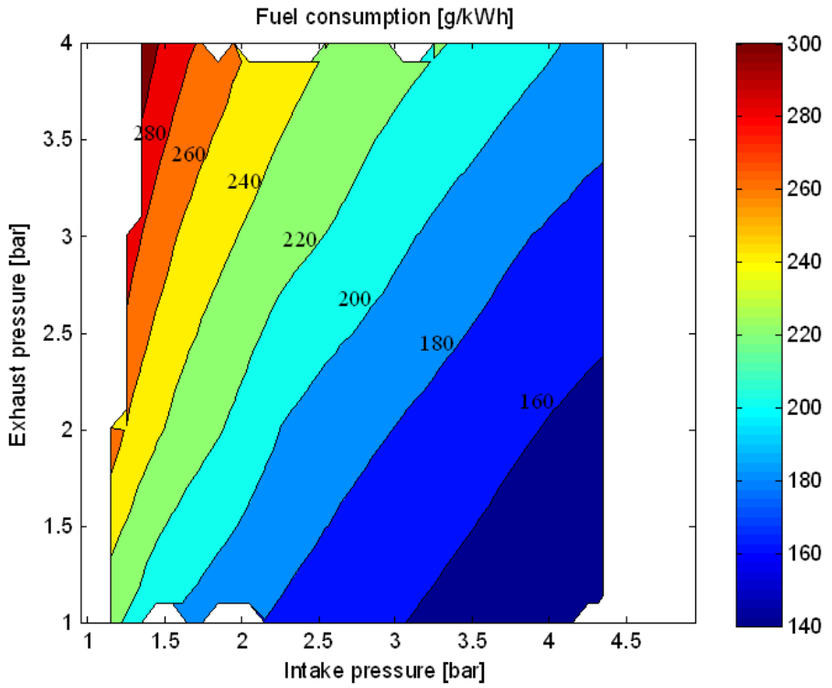

Fig. 13. Fuel consumption as a function of intake and exhaust pressures, for a fixed intake temperature of 25°C at BMEP = 10 bars

We present some qualitative explanations for this improvement, which will be completed with data in the rest of this paragraph. Actually, two main reasons are behind the fuel consumption reduction when the intake pressure is increased and exhaust pressure decreased:

- The scavenging work, called also "the low pressure cycle work", increases and turns out to be positive (motor). That is added to the work provided by the high pressure cycle and reduces fuel consumption. In a classic turbocharged Diesel, intake pressure is slightly lower than exhaust pressure; the scavenging work is slightly negative and requires more fuel for the same total work of the thermodynamic cycle.
- The high-pressure cycle efficiency increases with pneumatic hybridization thanks to higher fresh air quantity. This improvement is mainly due to lower thermal losses, due to the reduction of combustion temperature resulting from less fuel burned from one side, and higher air density (therefore higher calorific capacity) from the other side.

As mentioned before, the maximum pressure allowed in the cylinder limits the amount of intake pressure. Figure 14 shows the variation of the maximum cylinder pressure as a function of the intake and exhaust pressures. We observe the maximum cylinder pressure is almost not affected by exhaust pressure but varies linearly with intake pressure with a high slope of about 40 to 1. With a 4 bars intake pressure, the maximum cylinder pressure reaches already 180 bar.

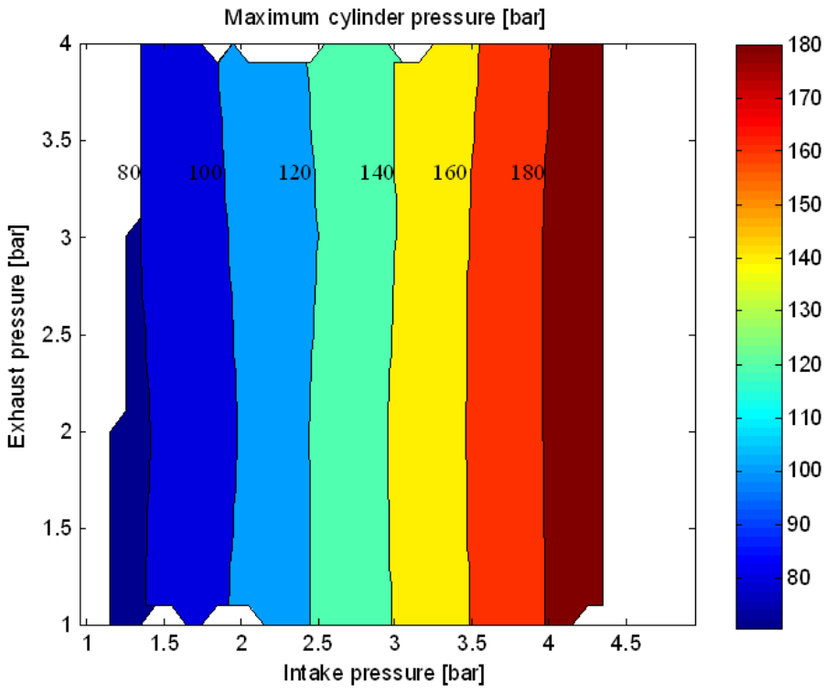

Fig. 14. Maximum gas pressure variation with intake and exhaust pressures, for a fixed intake temperature of 25°C, at BMEP = 10 bars

The second potential limitation that we have investigated is the exhaust temperature. Actually, exhaust valve has a threshold in terms of gas temperature not to be exceeded. As we can observe in Figure 15, the exhaust temperature is lower when intake pressure is

increased or exhaust pressure is decreased. Therefore, exhaust temperature will not limit the pneumatic hybridization.

After the analysis of the effect of intake and exhaust pressures for a fixed intake temperature and fixed injection advance, we illustrate (Figure 16) the effect of intake temperature and pressure on fuel consumption, for a fixed exhaust pressure of 1 bar and a fixed injection advance of 6 degrees. Fixing exhaust pressure to 1 bar assumes that the turbocharger is already by-passed. Fuel consumption is reduces as intake temperature lowers. As will be shown later with additional data, reducing intake temperature for the same intake pressure will reduce heat losses as well and improve cycle efficiency because the global gas temperature is lower (higher air density and lower initial cycle temperature).

Regarding maximum cylinder pressure, we observe in Figure 17 that reducing the intake temperature for the same intake pressure increases the maximum cylinder pressure. This is due to higher air quantity admitted. Therefore the maximum intake pressure we can reach is lower for low intake temperature. For example, at -50°C intake temperature, the maximum cylinder pressure reaches 180 bars for an intake pressure of 3.2 bars, which is 0.8 bars lower than the limitation at +25°C intake temperature.

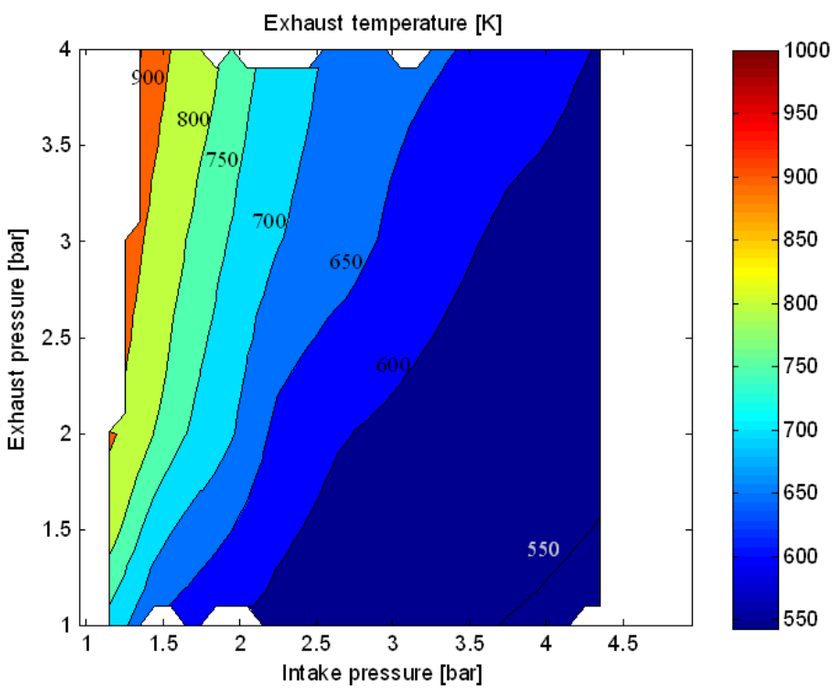

Fig. 15. Exhaust gas temperature function of intake and exhaust pressures, for a fixed intake temperature of 25°C, at BMEP = 10 bars

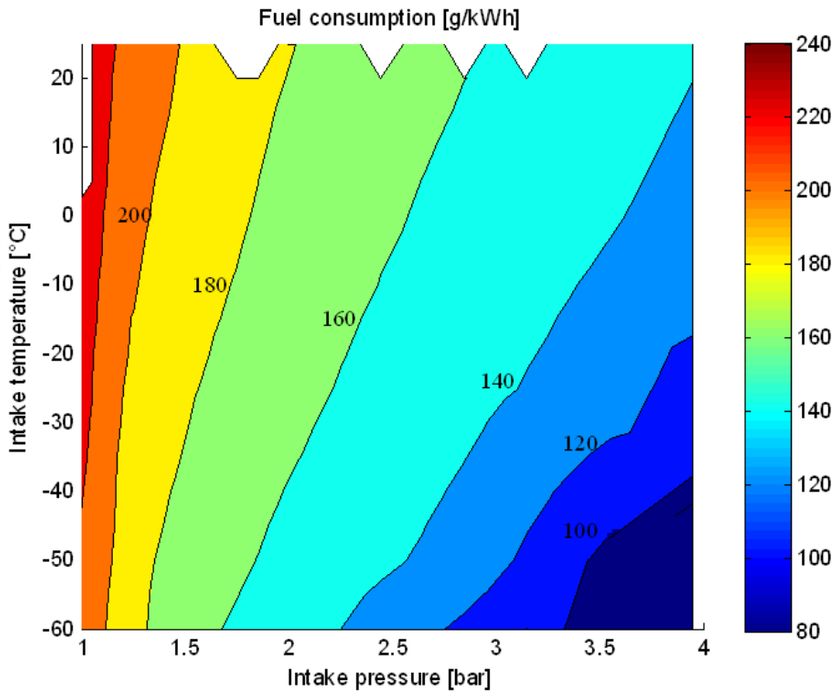

Fig. 16. Fuel consumption as a function of intake pressure and temperature, for a fixed exhaust pressure of 1 bar, at BMEP = 10 bars

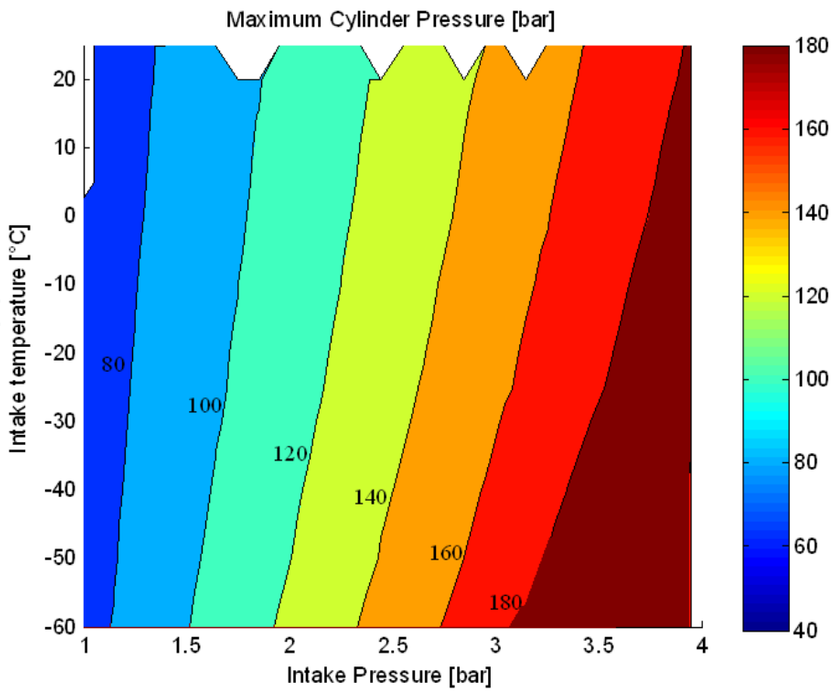

Fig. 17. Maximum gas pressure function of intake pressure and temperature, for a fixed exhaust pressure of 1 bar, at BMEP = 10 bars

The last parameter studied is the Injection Advance (IA) which is responsible of Start of Combustion (SOC) angle. Actually, there is an optimal advance that reduces the fuel consumption to a minimum, for every condition of intake pressure, intake temperature and exhaust pressure. The reasons are:

- The Auto-Ignition Delay (AID) depends of the intake conditions and so does the SOC because it is simply equal to the difference between the IA and the AID. It is important to have a SOC angle nearly before the Top Dead Center (TDC) in order to have good cycle efficiency.
- The thermal loss depends of the intake temperature and pressure and the cylinder pressure profile changes consequently. To have optimal cycle efficiency, the SOC needs to be adjusted around its nominal value.

For the simplification of the study, the AID was not modeled and the effect of the SOC angle is directly studied and set to its optimal value. Figure 18 illustrates the effect of SOC angle on fuel consumption, for the three chosen operating points. We observe that the optimal SOC angle for turbocharged mode is 6 degrees, for CAES charged at 25°C mode is 7 degrees and for CAES charged at -50°C mode, is 9 degrees. It is important to note that increasing injection advance to reduce fuel consumption, increases the maximum cylinder pressure, and therefore decreases the maximum intake pressure. In that case, the fuel consumption may increase instead of decreasing, but the global efficiency is better because less compressed air is consumed.

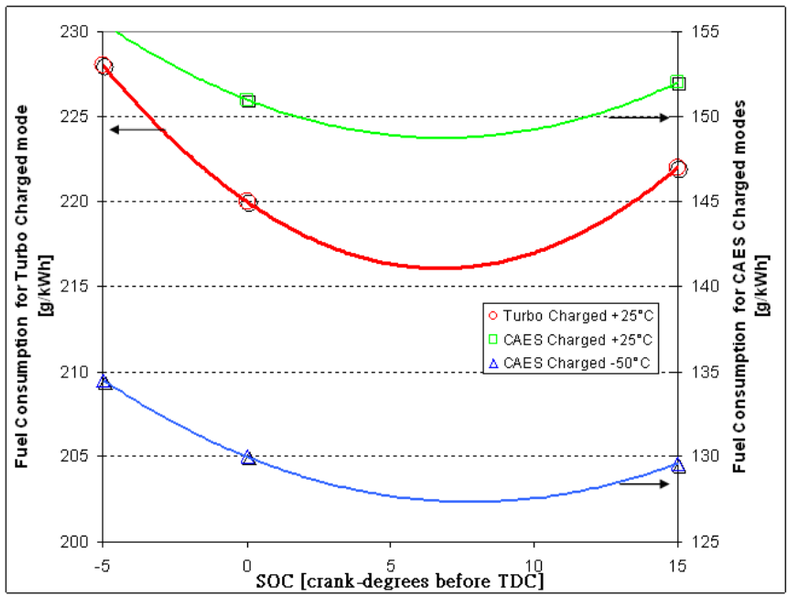

Fig. 18. Effect of SOC angle on fuel consumption, at BMEP = 10 bars, for different charging modes

The thermodynamic cycles of the chosen operating points are illustrated in Figures 19 and 17. All three operating modes are working at optimal SOC angles and therefore optimal IA.

Figure 19 illustrates the P-V diagram plotted in a logarithmic scale. It is interesting to analyze the low-pressure cycle called also the scavenging cycle. We notice that the pneumatic work witch is the area of the scavenging cycle is near zero for turbo-charged

mode and positive for CAES charged modes. We also notice that the scavenging work in CAES+25°C is slightly higher than the one in CAES-50°C because intake pressure is higher.

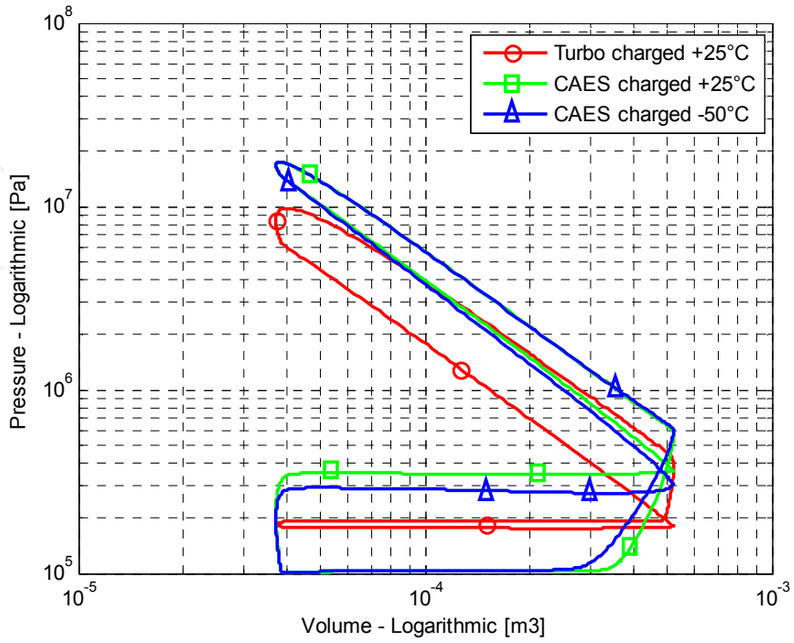

Fig. 19. log P-log V diagrams at BMEP=10 bars, for different charging modes

We notice in Figure 20 the high increase of the maximum cylinder pressure when moving from turbocharged mode to CAES charged mode.

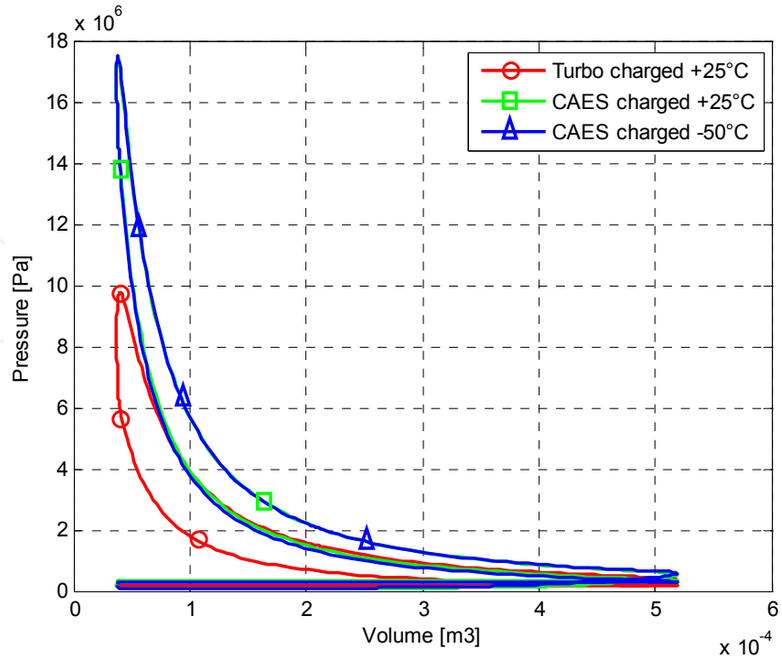

Fig. 20. P-V diagram at BMEP=10 bars, for different charging modes

Figure 21 and 22 illustrate respectively the T-θ diagram and heat exchange through boundaries for the three modes. We can see in Figure 21 that a significant decrease in gas temperature is obtained when moving from turbocharged mode to CAES-50°C mode passing by CAES+25°C charging mode. This temperature decrease is a result of the three following reasons:

1. The higher air density resulting from the higher intake pressure and/or the lower intake temperature, leads to higher calorific capacity of the in-cylinder gas and therefore lower temperature rise for a certain heat energy released by the combustion.
2. Lower heat release resulting from lower quantity of burned fuel that reduces temperature rise for CAES 25°C and CAES -50°C;
3. Intake air temperature is 75°C lower for CAES -50°C that is responsible for lower average gas temperature of this operating mode compared to CAES 25°C.

In Figure 22, negative flow means the gas is loosing energy through boundary and positive flow means the gas is earning energy from boundary. For turbocharged mode, the flow is positive only during intake because gas temperature at this time is lower than boundaries' temperatures. During combustion, expansion and exhaust phases, the heat flow is negative causing significant loss in energy. As for the CAES charged mode at 25°C, we observe that heat loss decreases significantly comparing to turbocharged mode but the flow is still negative. In CAES charged mode at -50°C, the overall heat flow is positive therefore the system is not loosing energy, on the contrary, it is recovering thermal energy from the engine. Of course, this assumes that the engine is hot and that the CAES charged mode at -50°C occurs occasionally, after a certain time of working under standard turbocharged mode. The thermal inertia of the Diesel engine defines the minimal and maximal working time of turbocharged mode and CAES mode respectively in order to make this hypothesis valid. In case the time of operating with CAES charged mode at -50°C exceeds a certain limit, the heat flow will stabilize to meet a global value near zero which will increase the fuel consumption by a small amount.

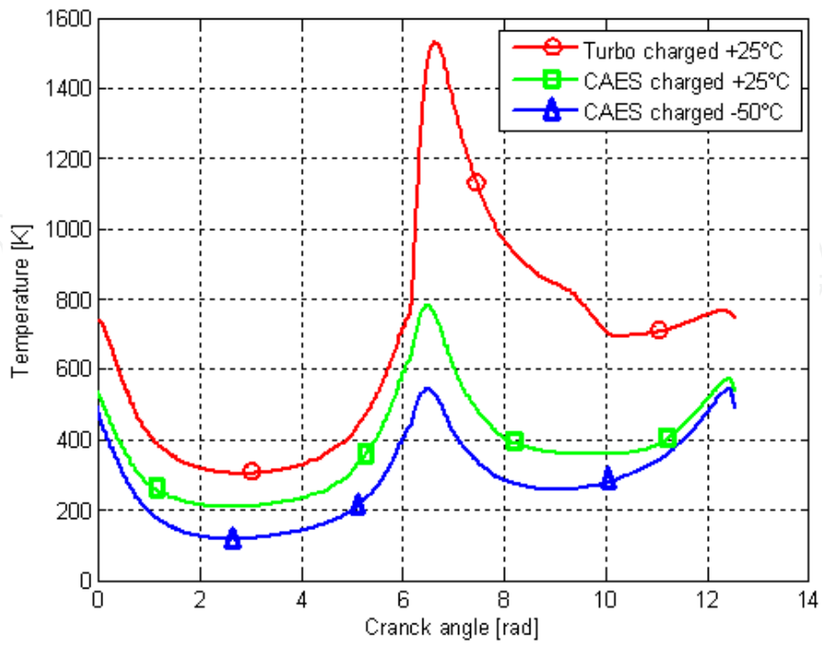

Fig. 21. T-θ diagram at BMEP=10 bars, for different charging modes

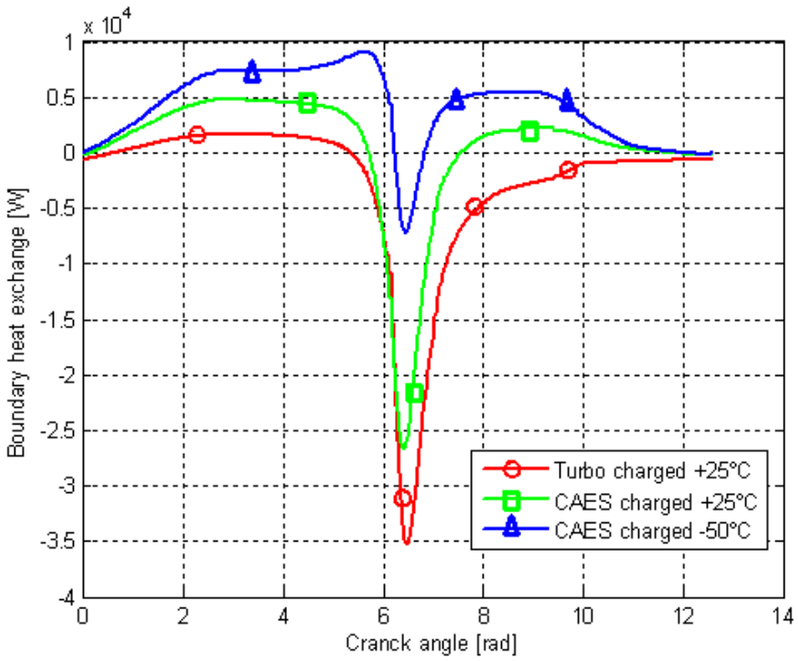

Fig. 22. Heat flow through boundary, for different charging modes, at BMEP = 10 bars

As a synthesis of this complete study around the operating point of BMEP 10 bars, Figure 23 illustrates the reasons for fuel economy brought by CAES charged modes compared to turbocharged mode. We observe that 65% of the fuel consumption reduction from turbocharged mode at +25°C to CAES charged mode at +25°C is caused by direct pneumatic power production and 35% is caused by heat loss reduction. The heat loss reduction constitutes the only reason for the improvement from CAES charged +25°C to CAES charged -50°C mode, as the pneumatic contribution is higher in CAES+25°C mode due to higher intake pressure.

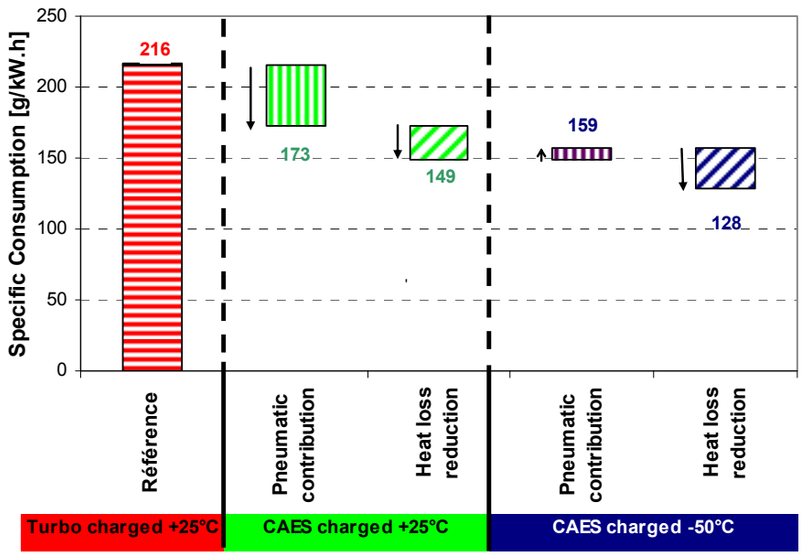

Fig. 23. Explanation of consumption change from a charging mode to another, at BMEP=10 bars

Optimization result at different loads

In this section, we will compare different charging modes on different criteria, for different operating points, after optimization. The charging modes considered are:

- CAES Charged mode at 50°C;
- CAES charged mode at 25°C;
- CAES charged mode at 0°C;
- CAES Charged mode at -50°C;
- Turbo charged mode at 25°C.

All CAES charged modes are operating at maximum allowable intake pressure, that is intake pressure for witch maximum gas pressure during thermodynamic cycle reaches 180 bars and at an exhaust pressure of 1 bar, while turbocharged mode operates at an intake pressure and exhaust pressure both dependant on BMEP but almost equal. All operating points are set with an optimal injection advance, the one that maximizes the cycle efficiency, even if the intake allowed pressure has to be decreased. As mentioned before, the variation of intake pressure and exhaust pressure as a function of BMEP for a turbocharged engine depends on the design of the turbocharger. We have taken here an example provided by a previous simulation [1] conducted on a Diesel engine.

Figure 24 illustrates the intake pressure and the injection advance at every operating point simulated. We can see that for higher loads the allowable intake pressure lowers; we can also see that a lower intake temperature will reduce the allowable intake pressure.

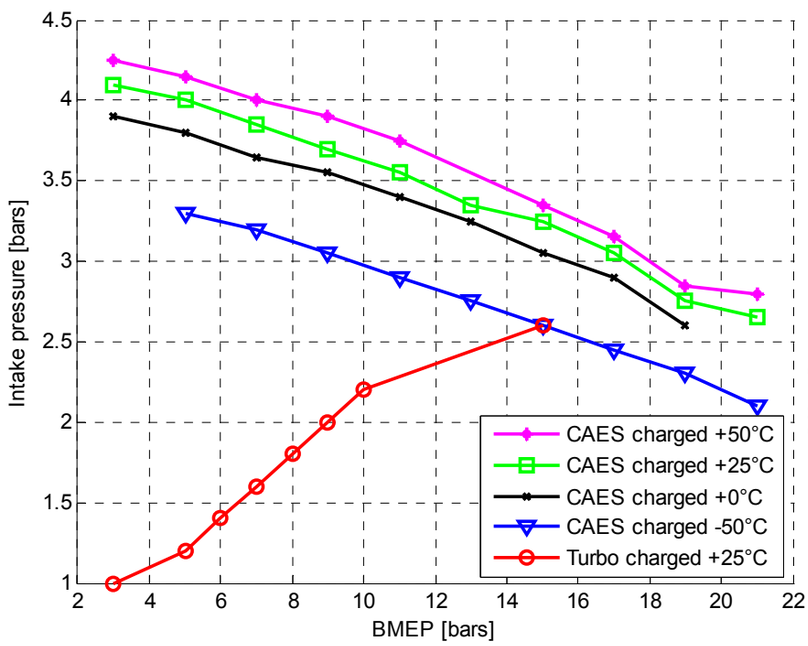

Fig. 24. Intake maximum pressure for different charging modes, function of engine load

These intake pressures make the maximum gas pressure during Diesel cycle reach 180 bars, as shown in Figure 25, while in turbocharged mode, maximal pressure is significantly lower.

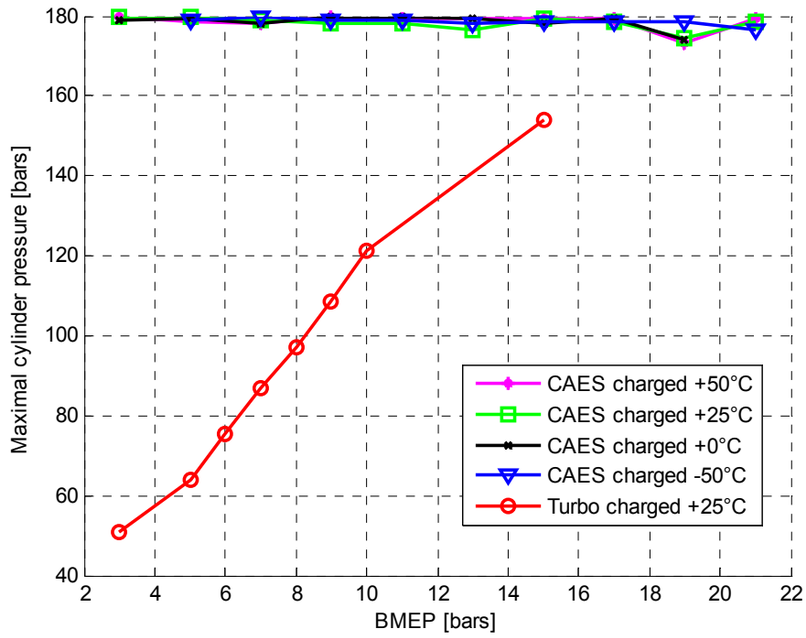

Fig. 25. Maximum cylinder pressure for different charging modes, function of engine load

When comparing fuel consumption of CAES charged mode with turbocharged mode, we observe in Figure 26 that at lower loads, the reduction is higher. That is due to the more important absolute pneumatic power as intake pressure is higher, relatively to the total power of the engine. We notice also that better fuel economy for lower intake temperature for the same reasons as described in the previous paragraph.

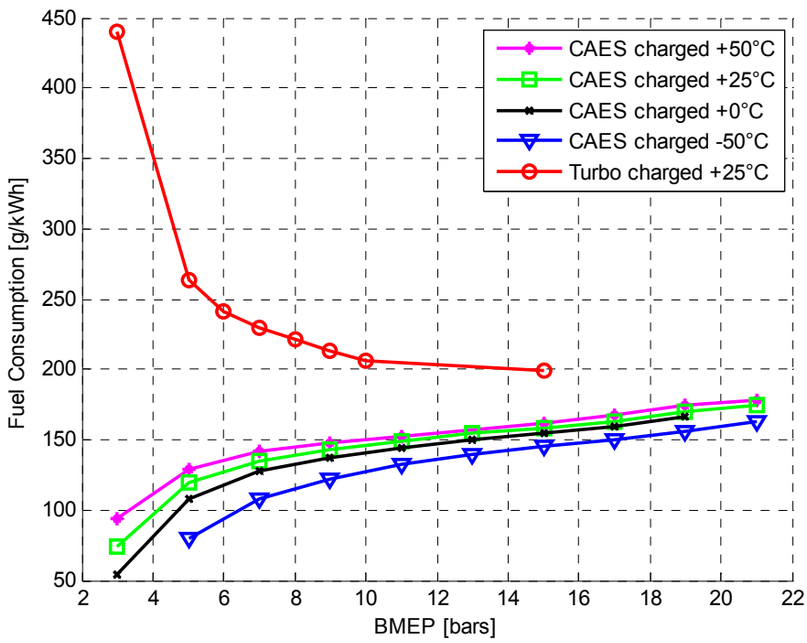

Fig. 26. Fuel specific consumption for different charging modes, function of engine load

Finally, the air consumption is one important criterion as the storage tank volume depends on it. Figure 27 shows that air consumption increases at low loads and also at low temperature because filling is better. In order to optimize the use of stored air, another criterion is necessary. We have calculated and illustrated in Figure 28, the fuel economy per kilogram of air consumed. This criterion has to be maximized in order to get the maximum advantage of stored air. As we can notice at Figure 28, it is more interesting to use CAES charged mode at low and very low loads. We can also see that even if it has positive effect on fuel consumption, very low intake air temperature is less suitable when considering consumed air quantity.

In case the storage pressure is higher than the intake temperature, it is needed therefore to expand it before introducing it into the engine intake. A temperature drop will probably accompany this expansion. In that case, we recommend heating the air after its expansion, using a free of charge source as the engine cooling system or an exhaust gas exchanger.

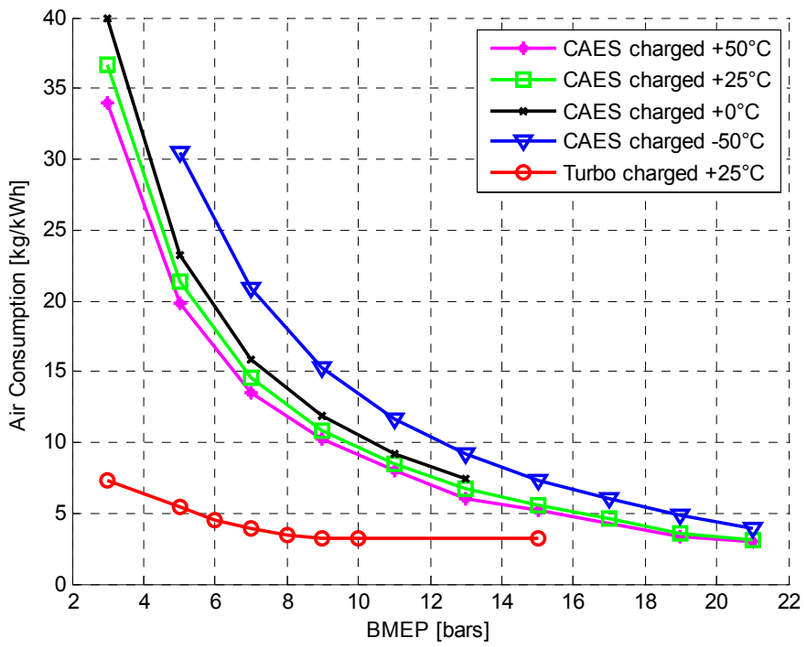

Fig. 27. Air specific consumption for different charging modes, function of engine load

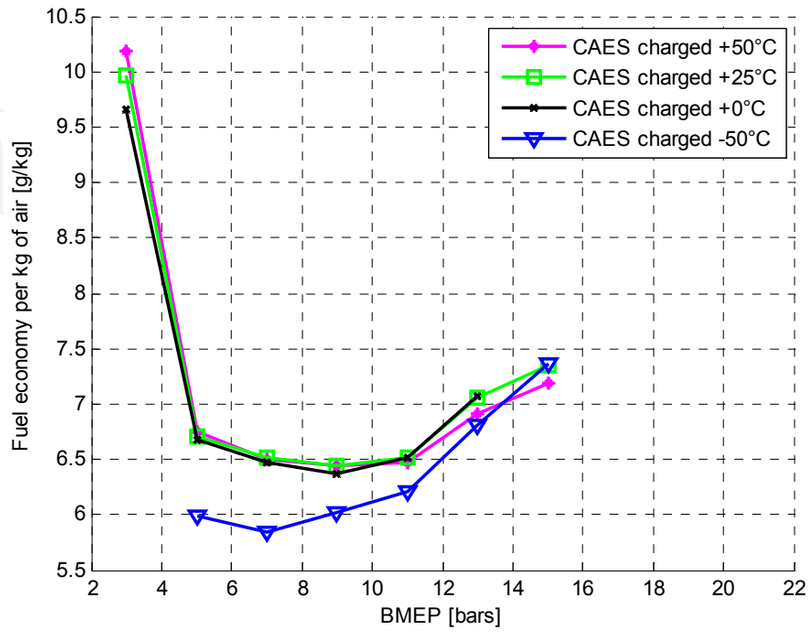

Fig. 28. Fuel economy per kilogram of air consumed, for different CAES charging modes, function of engine load

4. General conclusion and auto-critique

This document is a milestone study to demonstrate the interest around the WDCAS in portraying its potential to reduce fuel consumption and increase the efficiency of the diesel engine. We demonstrated that we can expect savings which can reach 50%. However, physical limits can jeopardise the achievement to this level of economy. Among these limits, we quote mainly those due to the permeability limit of the intake valves if a sound blocking takes place. Most, if the supercharging pressure is important Furthermore, some models used, were the object of validation in previous publications. In the case of our present study, we extrapolate the use of these models in zones beyond those in which they were validated. Among these models, the most important one being the engine performance (efficiency) according to the Air-to-Fuel ratio and which proposes appropriate sizing and representation of the gain in consumption that we forecasted. It is therefore necessary to either verify their validation in these conditions, or substitute more physical models (example: simulation of the thermodynamic cycle instead of using a polynomial model).

However, it has been demonstrated that when the intake pressure increases of 1 bar, maximal cylinder gas pressure increases about 40 bars. Considering that this maximal cylinder gas pressure needs to stay below a certain threshold for reliability reasons, the intake pressure is limited to 4 bars for the low loads and 3 bars for the high loads, as shown in Figure 14. This is a very big problem because that means that we have two options:

- The storage pressure is around four bars, witch means the volume needed to have significant fuel economy would be very high
- The storage pressure is high enough to have acceptable volume, but the air is expanded before the intake.
  - If the expansion happens through an orifice, a very high temperature drop occurs; the gas looses its entropy, and the global efficiency (energy discharged/energy stored) would be very low.
  - If the expansion happens through an air motor or air turbine, then it would be more efficient to expand the air until atmospheric pressure without any pneumatic Hybridization of the Diesel engine.

Other concepts of pneumatic hybrid Diesel engine are being studied to solve this problem.

5. Nomenclature

p	Pressure
T	Temperature
u	Internal energy
h	Enthalpy
θ	Crank angle
V	Volume
Q	Flow
q	Heat
P	Power
η	Efficiency
N	Rotational speed
x	Faction
m	Mass
A	Area

6. References

[1] Liu W, Gu S, Qiu D. Techno-economic assessment for off-grid hybrid generation systems and the application prospects in China. http://www.worldenergy.org/wecgeis/publications/.

[2] Weis TM, Ilinca A. The utility of energy storage to improve the economics of windeDiesel power plants in Canada. Renewable Energy 2008;33(7):1544e57.

[3] La stratégie énergétique du Québec 2006e2015. L'énergie pour construire le Québec de demain. http://www.mrnf.gouv.qc.ca/energie/eolien.
[4] Hunter R, Elliot G. WindeDiesel systems e a guide to the technology and its implementation. Cambridge (UK): Cambridge University Press; 1994.
[5] Forcione A. Système jumelé éolien-Diesel aux Îles-de-la-Madeleine (Cap-aux-Meules) e Établissement de la VAN optimale. Institut de Recherche, Hydro-Québec, Février; 2004.
[6] HOMER v2.0 e the optimisation model for distributed power. NREL. www.nrel.org.
[7] Ibrahim H, Ilinca A, Perron J. Solutions actuelles pour une meilleure gestion et intégration de la ressource éolienne. CSME/SCGM Forum 2008 at Ottawa. The Canadian Society for Mechanical Engineering, 5e8 June 2008.
[8] ACÉÉ. Association canadienne de l'énergie éolienne. http://www.canwea.com.
[9] Maisson JF. Wind power development in sub-arctic conditions with severe rime icing. In: Presented at the circumpolar climate change summit and exposition, Whitehorse, Yukon; 2001.
[10] www.nunavutpower.com.
[11] Reeves B. Kotzebue electric association wind projects. In: Proceedingsof NREL/AWEA 2002 windeDiesel workshop, Anchorage, Alaska, USA, 2002.
[12] Singh V. Blending wind and solar into the Diesel generator market. Renewable Energy Policy Project (REPP) research report, Winter 2001, No. 12, Washington, C.
[13] Reid R. Application de l'éolien en réseaux non reliés. Liaison Énergie-Francophonie,N_35/2e Trimestre; 1997.
[14] Jean Y, Nouaili A, Viarouge P, Saulnier B, Reid R. Développement d'un système JEDHPSS représentatif d'un village typique des réseaux non relies. Rapport IREQ-94-169-C; 1994.
[15] Gagnon R, Nouaili A, Jean Y, Viarouge P. Mise à jour des outils de modélisation et de simulation du Jumelage Éolien-Diesel à Haute Pénétration Sans Stockage et rédaction du devis de fabrication de la charge de lissage. Rapport IREQ-97- 124-C; 1997.
[16] www.danvest.com.
[17] Ilinca A, Chaumel JL. Implantation d'une centrale éolienne comme source d'énergie d'appoint pour des stations de télécommunications. Colloque international sur l'énergie éolienne et les sites isolées, Îles de la Madeleine; 2005.
[18] Ibrahim H, Ilinca A, Perron J. Energy storage systems e characteristics and comparisons. Renewable & Sustainable Energy Reviews 2008;12(5):1221-50.
[19] Ibrahim H, Ilinca A, Perron J. Comparison and analysis of different energy storage techniques based on their performance index. IEEE Canada, Electrical Power Conference 2007, "Renewable and alternative energy resources", EPC2007, Montreal, Canada, October 25-26, 2007.
[20] Belhamed M, Moussa S, Kaabeche A. Production d'électricité au moyen d'un système hybride éolien-photovoltaïque-Diesel. Revue Énergies Renouvelables: Zones Arides; 2002:49-54.

[21] Kaldellis JK, Vlachos GTh, Kavadias KA. Optimum sizing basic-principles of a combined photovoltaic windeDiesel hybrid system for isolated consumers. In: Proceedings of EuroSun 2002 international conference, Paper W141, Bologna, Italy, 2002.

[22] Bowen AJ, Cowie M, Zakay N. The performance of a remote wind-Diesel power system. Renewable Energy 2001;22(4):429-45.

[23] Ibrahim H, Younès R, Ilinca A. Optimal conception of a hybrid generator of electricity. CANCAM02007 ETS-39, Toronto, Canada. p. 358-9.

[24] Ibrahim H, Younès R, Ilinca A, Perron J. Investigation des générateurs hybrides d'électricité de type éolien-air comprimé. Colloque international des energies renouvelables E5, 04e05 mai 2007, Oujda MAROC.

[25] Robb D. Making a CAES for wind energy storage. North American Wind Power, June 2005.

[26] Ibrahim H, Ilinca A, Perron J. Moteur Diesel suralimenté, bases et calculs, cycles réel, théorique et thermodynamique. Rapport interne, UQAR-UQAC, LREE-02; Novembre 2006.

[27] Ibrahim H, Ilinca A, Younès R, Perron J, Basbous T. Study of a hybrid wind-Diesel system with compressed air energy storage. IEEE Canada, electrical power conference 2007, "Renewable and alternative energy resources", EPC2007, Montreal, Canada, October 25e26, 2007.

[28] Ibrahim H, Younès R, Ilinca A, Dimitrova M, Perron J. Study and design of a hybrid wind-Diesel-compressed air energy storage system for remote areas; Applied Energy 2010;87(5):1749e62.

[29] Basbous T. Étude de faisabilité d'un jumelage éolien-Diesel avec stockage ; d'énergie sous forme d'air comprimé. Mémoire de Maîtrise en ingénierie,Université du Québec à Rimouski, Août 2008.

[30] Garrett engine boosting systems. http://www.egarrett.com/.;

[31] Lallemand A. Modélisation d'un groupe turbocompresseur de suralimentation ; de moteur alternatif. Entropie 1983;111

[32] Parois A. Suralimentation par turbocompresseur. Techniques de l'ingénieur. Fascicule 1990;2631.

[33] Gissinger G, Le Fort-Piat N. Contrôle-Commande de la voiture. Hermes &Lavoisier; 2002.

[34] Dovifaaz X. Modélisation et commande d'un moteur Diesel en vue de la réduction de ses émissions. Thèse de doctorat, École Centrale de Lyon, France; 2001.

[35] Younes R, Ouladsine M, Noura H. Optimisation du débit d'air dans le Diesel suralimenté. Bordeaux, France: Congrès International Francophone d'Automatique,CIFA; 2006.

[36] Jensen JP, Kristensen AF, Sorenson SC, Hendricks E. Mean value modelling of a small turbocharged Diesel engine. SAE Technical paper, n_910070; 1991.

[37] Younes R. Élaboration d'un modèle de connaissance du moteur Diesel avec turbocompresseur à géométrie variable en vue de l'optimisation de ses émissions. Thèse de doctorat, École Centrale de Lyon, France; 1993.

[38] Kao M, Moskwa JJ. Turbocharged Diesel engine modeling for nonlinear engine control and state estimation. Journal of Dynamic Systems, Measurement, and Control 1995;117(1):20-30.
[39] Hendricks E. Continuous identification of a four stroke SI engine. In: Proc. Of the American control conference; 1990. p. 1876-81.
[40] Setoklosa H, Ferenc M, Osaba J, Osuch W. Evaluation of the dynamic response of a medium speed Diesel engine in generator set applied as stand-by power source for nuclear plants. In: CIMAC 87 in Warschau, 17th international congress on combustion engines; 1987.
[41] Hendrickes E. Mean value modeling of a small turbocharged Diesel engines. SAE paper n_910070; 1991.
[42] Younes R. Modélisation du turbocompresseur de suralimentation en régime stationnaire et instationnaire. DEA, École Centrale de Lyon, Ecully, France; 18 septembre 1989.
[43] Duyme V. Récupération énergétique à l'échappement d'un moteur de véhicule industriel par une turbine à gaz entraînant les auxiliaires, Simulation du fonctionnement et optimisation du système. Thèse de doctorat, INSA, Villeurbanne, France; 19 Février 1990.
[44] Ledger JD, Walmsley S. Computation and simulation of a turbocharged Diesel engine operation under transient load conditions. SAE paper n_71077; 1977.
[45] Heywood JB. Internal combustion engine fundamentals. 2nd ed. New York:McGraw-Hill; 1988. 950p.
[46] Millington BW, Hartles ER. Frictional losses in Diesel engine. SAE Transactions 1968;680590:2390e410.
[47] Winterbone DE, Tennant DWH. The variation of friction and combustion rates during Diesel engine transients. SAE paper; 1981, n_810339, 4p.
[48] Furuhama S, Sasaki S. New device for measurement of piston frictional forces in small engines. SAE Transactions 1983;831284:39-50.
[49] Yokooku K, Nagoa A, Oda H. Development of Mazda fuel-efficient concept car.SAE Transactions ;841309:295-307.
[50] Guichaoua JL, Magnien JF, Perrin H, Constants B. Frottement et temperature du film d'huile entre piston, segments et chemise d'un moteur Diesel. Journées internationales sur le moteur Diesel d'application. SIA École Centrale de Lyon, 13e14 mai 1984. p. 131-53.
[51] Gish RE, Mc-Cullough JD, Retzloff JB, Mueller H. Determination of engine friction. SAE Transactions 1958;66(9):649e-67.
[52] Omran R, Younes, Champoussin JC. Optimal control of Diesel engines: applications and methods. In: 3rd international conference on advances in vehicle control and safety, Argentina, 2007.
[53] Omran R, Younes, Champoussin JC. Optimization, genetic algorithm for dynamic calibration of engine's actuators. SAE paper, n_ 2007-01-1079.
[54] JANAF Thermochemical Tables, third edition, (1985)
[55] Woschni, G., 1967, A universally applicable equation for the instantaneous heat transfer coefficient in the internal combustion engine, SAE, 670 931.

[56] Stone, R., 1999, Introduction to internal combustion engines, Department of Engineering Science, University of Oxford
[57] Heywood, J.B., 1988, Internal Combustion Engine Fundamentals, New York, McGraw Hill.

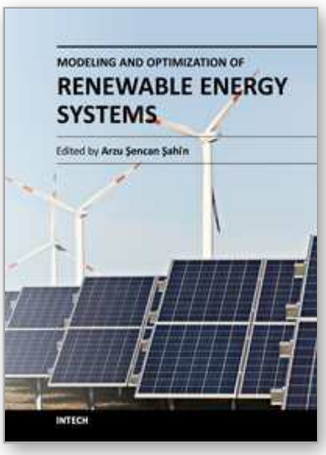

Modeling and Optimization of Renewable Energy Systems
Edited by Dr. Arzu Şencan

ISBN 978-953-51-0600-5
Hard cover, 298 pages
Publisher InTech
Published online 11, May, 2012
Published in print edition May, 2012

This book includes solar energy, wind energy, hybrid systems, biofuels, energy management and efficiency, optimization of renewable energy systems and much more. Subsequently, the book presents the physical and technical principles of promising ways of utilizing renewable energies. The authors provide the important data and parameter sets for the major possibilities of renewable energies utilization which allow an economic and environmental assessment. Such an assessment enables us to judge the chances and limits of the multiple options utilizing renewable energy sources. It will provide useful insights in the modeling and optimization of different renewable systems. The primary target audience for the book includes students, researchers, and people working on renewable energy systems.

InTech Europe
University Campus STeP Ri
Slavka Krautzeka 83/A
51000 Rijeka, Croatia
Phone: +385 (51) 770 447
Fax: +385 (51) 686 166
www.intechopen.com

InTech China
Unit 405, Office Block, Hotel Equatorial Shanghai
No.65, Yan An Road (West), Shanghai, 200040, China
中国上海市延安西路65号上海国际贵都大饭店办公楼405单元
Phone: +86-21-62489820
Fax: +86-21-62489821

IntechOpen